A New Series of Complex Perovskites $La_{1-x}Sr_xCr_{1-x}Ti_xO_3$: Structural Characterization

Roger H. Mitchell[1] and Anton R. Chakhmouradian

Department of Geology, Lakehead University, 955 Oliver Road, Thunder Bay, Ontario, Canada P7B 5E1

A new series of complex perovskite-type compounds $La_{1-x}Sr_xCr_{1-x}Ti_xO_3$ involving substitutions at both *A* and *B* sites was prepared by the ceramic technique (final heating at 1350°C). X-ray powder diffraction and profile-refinement study of this series show it to comprise orthorhombic perovskites (*Pbnm*, $a \approx b \approx \sqrt{2}a_p$, $c \approx \sqrt{2}a_p$, $Z = 4$) in the range $0 \le x \le 0.7$ and tetragonal perovskites (*I4/mcm*, $a \approx \sqrt{2}a_p$, $c \approx 2a_p$, $Z = 4$) in the range $0.8 \le x \le 0.9$. The tetragonal to cubic phase transition occurs between $x = 0.9$ and 1.0. Cation ordering is not observed in this solid solution series. The structures of the orthorhombic and tetragonal members are derived from the cubic aristotype by rotation of $(Cr,Ti)O_6$ octahedra. In contrast to most *Pbnm*-type perovskites, the orthorhombic compounds in the series $La_{1-x}Sr_xCr_{1-x}Ti_xO_3$ have $a > b$, possibly resulting from distortion of the octahedra. © 1999 Academic Press

INTRODUCTION

Perovskite-type compounds of the general formula $LaB^{3+}O_3$ (B = Cr, Mn, Fe, Co, Ni, Ru) have been extensively studied recently as prospective catalysts (1, 2). High catalytic oxidation activities and relative ease of manufacturing make these compounds a potential anode material for solid-oxide fuel cells (1, 3). It has been demonstrated in a number of studies that catalytic activities of $LaB^{3+}O_3$-type phases can be significantly improved by cationic substitutions at the A or B sites in the perovskite lattice (1, 2, 4). For example, substitution of La by Sr at the A site and accommodation of easily reducible transition metals at the B site normally increase catalytic activity of the material (1, 4). Previous experimental studies have concentrated on simple substitutions involving La and Sr or Cr plus another B-site cation (2, 5, 6). To our knowledge, no data are available on coupled A–B-site substitutions in $LaCrO_3$. On the basis of previously published experimental data (1, 4), we may expect that a coupled substitution involving Sr and Ti

would improve catalytic properties of $LaCrO_3$. Consequently, one of the objectives of the present study was to investigate solid solubility in the system $LaCrO_3$–$SrTiO_3$. The second objective was structural characterization of the members of this series using the X-ray powder diffraction (XRD) and Rietveld profile refinement techniques (7).

The results of the present study also have direct implications for the mineralogy of the earth's upper mantle, as it has been recently demonstrated (8) that perovskite-type compounds enriched in La plus other light rare-earth elements, Sr, and Cr occur as microinclusions in diamonds, and are probably derived from geochemically altered regions in the mantle. In these regions, commonly referred to as metasomites, perovskite-type phases may be one of the major hosts for the rare elements, including light lanthanides (*Ln*), Sr, Nb, and Th. Pure members of the solid solution $La_{1-x}Sr_xCr_{1-x}Ti_xO_3$ have not been encountered in nature, as the enrichment in La and Sr is invariably accompanied by high contents of alkalies. Thus, most naturally occurring compositions show extensive solid solutions toward $Na_{1/2}Ln_{1/2}TiO_3$ and $K_{1/2}Ln_{1/2}TiO_3$. However, as much as 18 mol% $LaCrO_3$ and 38 mol% $SrTiO_3$ have been determined in the composition of diamond-hosted perovskite inclusions from South Africa (8). The very small size of these inclusions precludes their examination by XRD techniques; thus the problem of understanding compositional variation of mantle-derived perovskites must be approached on the basis of experimental data.

EXPERIMENTAL

Compositions corresponding to the end and intermediate members of the series $La_{1-x}Sr_xCr_{1-x}Ti_xO_3$ ($x = 0$, 0.1, 0.2, ..., 1.0) were synthesized from stoichiometric amounts of La_2O_3, $SrCO_3$, Cr_2O_3, and TiO_2 (high purity grade). The oven-dried reagents were mixed, ground in an agate mortar, and heated in air for 24 h initially at 1100°C and, after regrinding, for 24 h at 1350°C. After the final run, the samples were rapidly cooled in air to the room temperature. All synthesis products are powders with the color ranging

[1]To whom correspondence should be addressed. Fax: (807) 346–7853. E-mail: RMITCHEL@gale.lakeheadu.ca.

from dark green ($x = 0$) through greenish black and black to very pale pinkish gray ($x = 1.0$). The change in color to black with increasing Sr content may indicate partial oxidation of Cr^{3+} to Cr^{4+}, i.e., some deviation from the binary solid solution $LaCrO_3$–$SrTiO_3$ toward the ternary system $LaCrO_3$–$SrTiO_3$–$SrCrO_3$.

The size of crystals in the powders does not exceed 10–15 μm; thus, the Rietveld method (6) was used for structural characterization of the synthesized compounds. XRD powder patterns of the synthesis products were obtained on a Philips 3710 diffractometer ($T = 20°C$; radiation $CuK\alpha$; 2θ range $10°$–$145°$; step $\Delta 2\theta$ $0.02°$; time per step 2 s). The XRD patterns were analyzed by the Rietveld method using the FULLPROF program (9). In most cases, the XRD patterns of the synthesis products comprise only diffraction lines characteristic of perovskite-type phases. For $x = 0.1$, 0.2, 0.4, and 0.8, the XRD patterns also include a weak diffraction line with $d = 3.25$ Å, which corresponds to the strongest reflection of rutile TiO_2 (ASTM 21-1276). A faint diffraction line with $d = 3.63$ Å on the pattern of $x = 0.2$ most probably corresponds to the (012) reflection of Cr_2O_3 (ASTM 38-1479). The intensity of these lines does not exceed 1.5–1.7% of the most intense perovskite line [(110) in the pseudocubic setting]. Given the small amount of TiO_2 in the synthesis products, it was not included in the refinement, and all patterns were refined in the one-phase mode. The range 10–$20°$ 2θ was excluded from the refinement, as it had significantly higher background intensities and proved not to contain any diffraction lines.

RESULTS AND DISCUSSION

End Members

$LaCrO_3$ was first synthesized by Geller (10) and shown to be isostructural to orthorhombic perovskite $GdFeO_3$. The unit-cell parameters obtained by Geller (10) show the axis ratio typical of most other $Pbnm$-type perovskites, i.e., $a < c/\sqrt{2} < b$. The crystal structure of room-temperature form of $LaCrO_3$ was subsequently refined in the orthorhombic symmetry by profile fitting of neutron powder diffraction data (11). In contrast to most $Pbnm$-type perovskites (e.g., $GdFeO_3$, $CaTiO_3$, and $NaMgF_3$), Khattak and Cox used a setting in which a is greater than b, as the refinement in such a setting converged to a better R_I (11). To resolve this controversy, we tried both possible axis orientations ($a < b$ and $b < a$) within the same $Pbnm$ cell. In our refinement of $x = 0$, we also obtained a significantly better fit to the latter model ($R_I = 7.0$ vs $R_I = 9.1$). Most importantly, careful analysis of minor reflections shows that the Khattak and Cox's model achieves a better correspondence with the observed XRD pattern (Fig. 1). The unit-cell parameters and atomic coordinates obtained for $LaCrO_3$ in the present work are in a reasonable agreement with those reported in the previous studies (5, 10, 11) (Table 1).
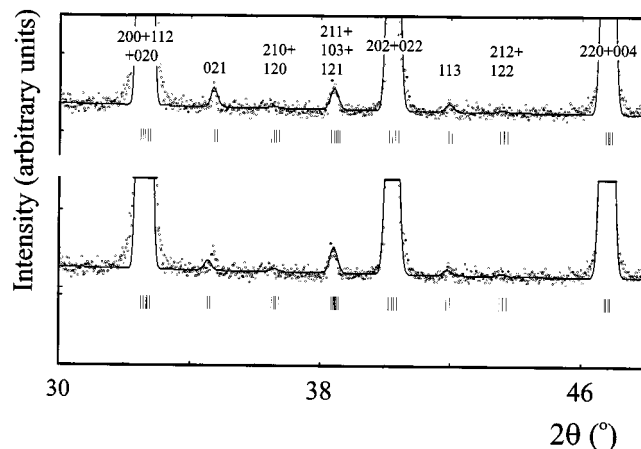
FIG. 1. Calculated (line) and observed (dots) XRD patterns for $x = 0$. The upper pattern corresponds to the $Pbnm$ model with $a > b$ (11), the lower pattern to the "conventional" $Pbnm$ model ($b > a$). Note the better fit between the positions of the (021) peak in the observed pattern and the $Pbnm$ model with $a > b$.

At room temperature, $SrTiO_3$ has an undistorted cubic structure (space group $Pm\bar{3}m$) which is stable above 110 K (12). Consequently, the pattern of $SrTiO_3$ synthesized in the present work was refined in the $Pm\bar{3}m$ structural model with Ti at $1a$, Sr at $1b$, and O at $3d$ sites, respectively. The refinement was carried out to $R_I = 6.4\%$, and the refined unit-cell parameter [$a = 3.9052$ Å] is close to previously obtained values (e.g., ASTM 35-734).

Intermediate Members

Complete solubility was observed between the end members of the series $La_{1-x}Sr_xCr_{1-x}Ti_xO_3$. As demonstrated by

TABLE 1
$LaCrO_3$ ($x = 0$): Comparison with Previously Published Structural Data

	This study[a]	Khattak and Cox (11)[b]		This study[a]	Khattak and Cox (11)[b]
a (Å)	5.5163(1)	5.520			
b (Å)	5.4797(1)	5.483			
c (Å)	7.7588(2)	7.765			
La		O1			
x	−0.0026(5)	−0.0046(5)	x	0.059(3)	0.0676(4)
y	0.0191(2)	0.0196(4)	y	0.496(2)	0.4935(6)
z	1/4	1/4	z	1/4	1/4
B (Å^2)	0.64(2)	0.1(1)	B (Å^2)	0.4(4)	0.1(1)
Cr		O2			
x	1/2	1/2	x	0.228(3)	0.2265(3)
y	0	0	y	0.233(3)	0.2265
z	0	0	z	0.537(2)	0.5338
B (Å^2)	0.44(4)	−0.4(1)	B (Å^2)	1.3(3)	0.3(1)

[a]Profile refinement of X-ray powder diffraction data.
[b]Profile refinement of neutron powder diffraction data.

peak splitting, all intermediate members of this series deviate from the cubic symmetry. Importantly, no superlattice peaks resulting from the A- or B-site cation ordering in the perovskite lattice were observed. In the compositional range $0.1 \leq x \leq 0.6$, the XRD patterns can be indexed on the orthorhombic cell $Pbnm$ ($a \approx b \approx \sqrt{2}a_p$, $c \approx 2a_p$, $Z = 4$) identical to that established for the $LaCrO_3$ end member (Fig. 2). As in the case of $LaCrO_3$, we used the $Pbnm$ setting with the "reversed" axis ratio (see above). For $x = 0.7$, the peaks that may be used to distinguish between the "conventional" and "reversed" settings (e.g., 021) are virtually undetectable, and the pattern of this compound was refined on the basis of the same orthorhombic cell with $a > b$.

The refined atomic coordinates and isotropic thermal parameters for some orthorhombic members of the series $La_{1-x}Sr_xCr_{1-x}Ti_xO_3$ are given in Table 2. Selected interatomic distances and bond angles are listed in Table 3. Structurally, the orthorhombic perovskites obtained in this study are closely related to $GdFeO_3$ and $CaTiO_3$ (13, 14). These structures are derived from the ideal by tilting of BO_6 octahedra about [001] and [110] of the undistorted cubic cell. The tilting normally results in reduction of the coordination of an A-site cation (12 in the undistorted structure). In most orthorhombic perovskites, the coordination number of the A-site cation (CN_A) is 8 (15), but in some compounds with a relatively small B-site cation, it may reach the maximum value of 12 (e.g., $SmAlO_3$) (16). Theoretically, CN_A may vary between 8 and 12, depending on the tilt angle and ratio between ionic radii of the A- and B-site cations. For example, perovskites examined in this study have somewhat intermediate CN_A ranging between 9 and 10 (Table 3).

TABLE 2
$La_{1-x}Sr_xCr_{1-x}Ti_xO_3$: Crystallographic Characteristics for $x = 0.2$ and 0.4

Atom	Position	x	y	z	B (Å)
A^a	4c	0.000(2)	0.0135(3)	1/4	0.74(3)
		−0.005(3)	**0.0105(1)**		**0.80(3)**
B^b	4b	1/2	0	0	0.51(4)
					0.54(4)
O1	4c	0.029(1)	0.500(3)	1/4	1.2(8)
		0.046(7)	**0.504(4)**		**0.8(7)**
O2	8d	0.230(5)	0.237(5)	0.542(3)	0.5(4)
		0.236(6)	**0.227(4)**	**0.521(3)**	**0.8(4)**

Note. Final agreement factors and cell parameters ($Pbnm$) for $x = 0.2$: $R_p = 16.4$, $R_{wp} = 22.7$, $R_I = 6.5$, $\chi^2 = 1.68$, $a = 5.5117(5)$, $b = 5.4740(6)$, $c = 7.7735(9)$ Å; for $x = 0.4$: $R_p = 14.7$, $R_{wp} = 20.3$, $R_I = 6.6$, $\chi^2 = 1.63$, $a = 5.5104(4)$, $b = 5.4740(4)$, $c = 7.7940(6)$ Å.
$^a A = $ La, Sr; $B = $ Cr, Ti.
^{b} Values for $X = 0.4$ in boldface.

In the compositional range $0.8 \leq x \leq 0.9$, only a few diffraction lines with small d spacings [e.g., $(332)_p$] show splitting indicative of tetragonal symmetry. However, lines that could be used to distinguish between the two possible space groups $I4/mcm$ and $P4/mbm$ (hkl, where $l = $ odd) have very low intensity. Consequently, we tested both structural models, as well as the $Pbnm$ model, given that the true symmetry could still be orthorhombic. For both compounds, the best correspondence between calculated and observed diffraction data was obtained with the $I4/mcm$ model (Fig. 3). Results of the refinement for $x = 0.9$, as well as selected interatomic distances and angles, are given in
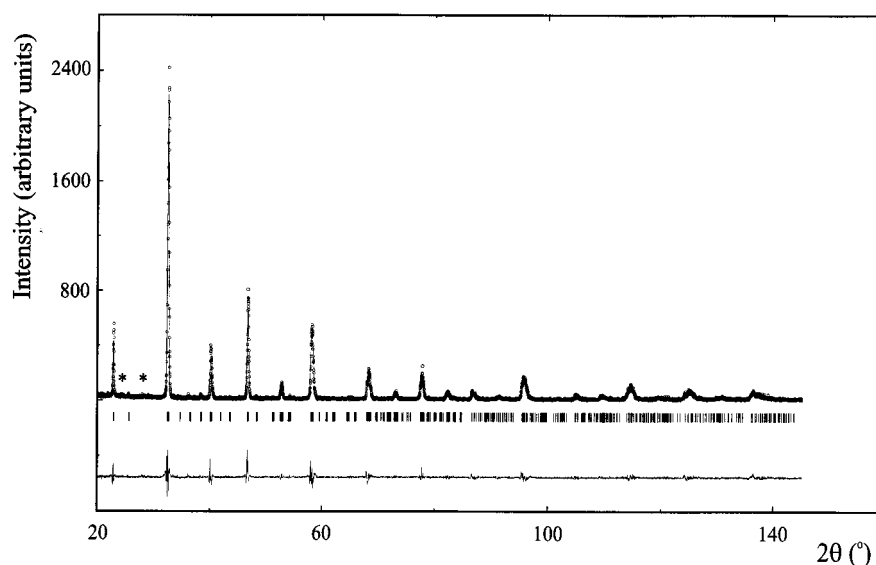
FIG. 2. Calculated (line) and observed (dots) XRD patterns and difference spectrum for $x = 0.2$. For the agreement factors see Table 2. Diffraction lines corresponding to (012) of Cr_2O_3 and (110) of TiO_2 are marked with asterisks.

TABLE 3
$La_{1-x}Sr_xCr_{1-x}Ti_xO_3$: Selected Interatomic Distances (Å) and Angles (°) for $x = 0.2$ and 0.4

	$x = 0.2$	$x = 0.4$		$x = 0.2$	$x = 0.4$
A^a–O1	2.394	2.528	O1–B–O1	180.0	180.0
A–O1	2.804	2.714	$2 \times$ O1–B–O2	86.2	88.8
A–O1	2.764	2.788	$2 \times$ O1–B–O2	87.8	89.8
A–O1	3.081	2.982	$2 \times$ O1–B–O2	92.2	90.2
$2 \times d$ A–O2	2.433	2.550	$2 \times$ O1–B–O2	93.8	91.2
$2 \times d$ A–O2	2.547	2.702	$2 \times$ O2–B–O2	88.2	89.1
$2 \times d$ A–O2	2.935	2.759	$2 \times$ O2–B–O2	180.0	180.0
$2 \times d$ A–O2	3.130	3.100	$2 \times$ O2–B–O2	91.8	90.9
$2 \times d$ B^b–O1	1.979	1.965	$2 \times$ O2–B–O2	180.0	180.0
$2 \times d$ B–O2	1.921	1.918	B–O1–B	158.4	165.1
$2 \times d$ B–O2	2.037	1.990	B–O2–B	157.8	167.3

$^a A = $ La, Sr; $B = $ Cr, Ti.

TABLE 4
$La_{1-x}Sr_xCr_{1-x}Ti_xO_3$: Crystallographic Characteristics, Selected Interatomic Distances (Å) and Angles (°) for $x = 0.9$

Atom	Position	x	y	z	B (Å^2)
A^a	$4c$	0	0	1/4	0.89(4)
B	$4b$	0	1/2	0	0.65(5)
O1	$4c$	0	1/2	1/4	0.6(4)
O2	$8h$	0.251(3)	0.751(3)	0	1.1(4)
$4 \times d$ A–O1	2.760		O1–B–O1		180.0
$4 \times d$ A–O2	2.754		O1–B–O2		90.0
$4 \times d$ A–O2	2.766		O2–B–O2		90.0
$2 \times d$ B–O1	1.952		O2–B–O2		180.0
$4 \times d$ B–O2	1.951		B–O1–B		180.0
			B–O2–B		179.5

Note. Final agreement factors and cell parameters ($I4/mcm$) for $x = 0.9$: $R_p = 14.6$, $R_{wp} = 19.5$, $R_I = 5.9$, $\chi^2 = 2.59$, $a = 5.5190(3)$, $c = 7.8086(8)$ Å.
$^a A = $ Sr, La; $B = $ Ti, Cr.

Table 4. The mean A–O and B–O distances (2.763 and 1.959 Å, respectively) are very close to their ideal values calculated from ionic radii of the corresponding elements (2.782 and 1.956 Å, respectively). Note that for $0.8 \leq x \leq 0.9$, the fractional coordinates of oxygen atoms at $8h$ are within the estimated standard deviation from the ideal values ($x = 0.25$, $y = 0.75$) corresponding to the undistorted cubic structure. Also, in contrast to the orthorhombic members of the series, those with the tetragonal symmetry exhibit a 12-fold coordination of Sr + La at the A site. This suggests that their structure deviates only slightly from the cubic aristotype.

The perovskite series $La_{1-x}Sr_xCr_{1-x}Ti_xO_3$ examined in this study is unusual, inasmuch as it involves two cationic substitutions with essentially opposite structural effect. At the A site, La^{3+} is substituted by significantly larger Sr^{2+} (1.36 and 1.44 Å, respectively), whereas at the B site, Cr^{3+} (0.615 Å) is replaced by smaller Ti^{4+} (0.605 Å) [ionic radii from Shannon (17)]. This results in a somewhat unusual pattern of unit-cell parameter variation (Fig. 4). However, the gradually increasing unit-cell volume (Fig. 4) demonstrates that the expansion caused by incorporation of Sr^{2+} into the structure outweighs the "shrinkage" effect caused by gradually decreasing B–O distance (from 1.969 Å for LaCrO$_3$ to 1.953 Å for SrTiO$_3$). Unit-cell parameters for all compositions are listed in Table 5.

Generally, octahedral tilting in orthorhombic and tetragonal perovskites results in a reduction of unit-cell
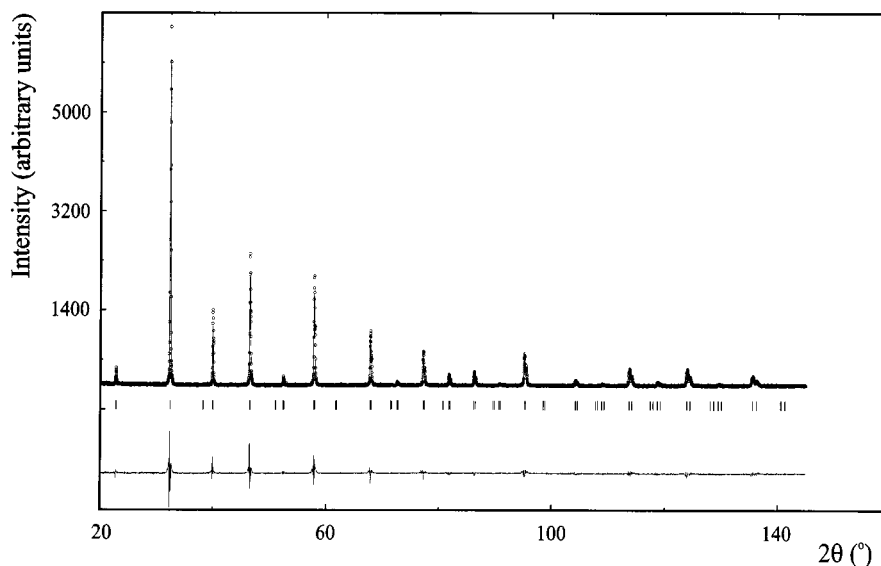
FIG. 3. Calculated (line) and observed (dots) XRD patterns and difference spectrum for $x = 0.9$. For the agreement factors see Table 4.
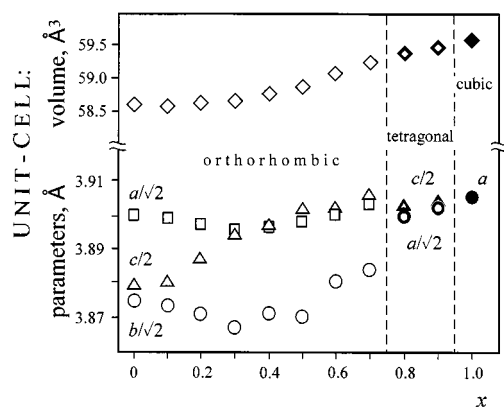
FIG. 4. La$_{1-x}$Sr$_x$Cr$_{1-x}$Ti$_x$O$_3$: variation of the unit-cell parameters (reduced to pseudocubic) with the composition.

parameters perpendicular to the axis of tilt. A parameter parallel to the axis of tilt remains unchanged. Therefore, angles of tilt can be roughly estimated by relating unit-cell parameters in the distorted structure, assuming regularity of the BO_6 octahedra (18). However, the "reversed" axis ratio in the orthorhombic perovskites La$_{1-x}$Sr$_x$Cr$_{1-x}$Ti$_x$O$_3$ precludes use of the equations conventionally applied for calculation of tilt angles from the unit-cell parameters (18). Inversion of the orthorhombic cell parameters a and b is commonly observed in perovskites approaching the transition point to a higher symmetry (rhombohedral or tetragonal), and may be induced by distortion of the BO_6 octahedra (P. M. Woodward, personal communication). Interestingly, the equations for tilt angles based on fractional coordinates of oxygen atoms and independent of the cell parameters give significantly different values for the same tilt components, which also seems to indicate some distortion of BO_6. The observed variation in the unit-cell

parameters (Fig. 4) suggests that the tilting reaches its maximum magnitude in the middle of the solid solution La$_{1-x}$Sr$_x$Cr$_{1-x}$Ti$_x$O$_3$. This is not an unexpected feature, given that the compositions $0.4 \leq x \leq 0.6$ host the greatest number of cations of different size and charge at both A and B sites.

CONCLUSIONS

Complete solubility is observed between LaCrO$_3$ (orthorhombic, $Pbnm$) and SrTiO$_3$ (cubic, $Pm\overline{3}m$). The intermediate members of the series La$_{1-x}$Sr$_x$Cr$_{1-x}$Ti$_x$O$_3$ are orthorhombic ($Pbnm$) up to $x = 0.7$ and tetragonal ($I4/mcm$) between $x = 0.8$ and 0.9. The unit-cell volume (reduced to the pseudocubic cell) gradually increases with x owing to the replacement of La^{3+} by larger Sr^{2+} cations. Cation ordering does not occur in this perovskite series; the structures of the orthorhombic and tetragonal members are derived from the ideal cubic lattice by tilting of (Cr,Ti)O$_6$ octahedra. The maximum distortion probably occurs in the middle of the solid solution ($x = 0.4$–0.6).

REFERENCES

1. H. Arai, T. Yamada, K. Eguchi, and T. Seiyama, *Appl. Catal.* **26,** 265 (1986).
2. J. G. McCarty and H. Wise, *Catal. Today* **8,** 231 (1990).
3. B. C. H. Steele, P. H. Middleton, and R. A. Rudkin, *Solid State Ionics* **40/41,** 388 (1990).
4. M. Stojanovic, H. Moudallal, A. J. Jacobson and C. A. Mims, *J . Catal.* **166,** 324 (1997).
5. M. Stojanovic, R. G. Haverkamp, C. A. Mims, H. Moudallal, and A. J. Jacobson, *J. Catal.* **165,** 324 (1997).
6. B. Gilbu, H. Fjellvag, and A. Kjekshus, *Acta Chem. Scand.* **48,** 37 (1994).
7. H. M. Rietveld, *J. Appl. Crystallogr.* **2,** 65 (1969).
8. M. G. Kopylova, R. S. Rickard, A. Kleyenstueber, W. R. Taylor, J. J. Gurney, and L. R. M. Daniels, *Russ. Geol. Geophys.* **38,** 405 (1997).
9. J. Rodriguez-Carvajal, "FULLPROF" Program: Rietveld Pattern Matching Analysis of Powder Patterns." ILL, Grenoble, 1990.
10. S. Geller, *Acta Crystallogr.* **10,** 243 (1957).
11. C. P. Khattak and D. E. Cox, *Mater. Res. Bull.* **12,** 463 (1977).
12. H. Unoki and T. Sakudo, *J. Phys. Soc. Japan* **23,** 546 (1967).
13. S. Geller, *J. Chem. Phys.* **24,** 1236 (1956).
14. S. Sasaki, C. T. Prewitt, J. D. Bass, and W. A. Schulze, *Acta Crsytallogr. Sect. C* **43,** 1668 (1987).
15. P. M. Woodward, *Acta Crystallogr. Sect. B* **53,** 44 (1997).
16. M. Marezio, P. D. Dernier, and J. P. Remeika, *J. Solid State Chem.* **4,** 11 (1972).
17. R. D. Shannon, *Acta Crystallogr. Sect. A* **32,** 751 (1976).
18. H. D. Megaw, "Crystal Structures: A Working Approach," Saunders, Philadelphia, 1973.

TABLE 5
La$_{1-x}$Sr$_x$Cr$_{1-x}$Ti$_x$O$_3$: Variation of Unit-Cell Parameters (Å)

x	a	b	c
	Orthorhombic ($Pbnm$)		
0	5.5163(1)	5.4797(1)	7.7588(2)
0.1	5.5145(4)	5.4779(4)	7.7603(6)
0.2	5.5117(5)	5.4740(6)	7.7735(9)
0.3	5.5088(4)	5.4685(5)	7.7884(9)
0.4	5.5104(4)	5.4740(4)	7.7940(6)
0.5	5.5133(4)	5.4724(4)	7.8039(5)
0.6	5.5161(3)	5.4875(4)	7.8057(4)
0.7	5.5204(3)	5.4932(4)	7.8124(4)
	Tetragonal ($I4/mcm$)		
0.8	5.5151(5)		7.807(2)
0.9	5.5190(3)		7.8086(8)
	Cubic ($Pm\overline{3}m$)		
1.0	3.90520(4)		